



**HAL**  
open science

## **A generic power wheelchair lumped model in the sagittal plane: towards realistic self-motion perception in a virtual reality simulator**

Fabien Grzeskowiak, Ronan Le Breton, Louise Devigne, François Pasteau, Marie Babel, Sylvain Guégan

### ► **To cite this version:**

Fabien Grzeskowiak, Ronan Le Breton, Louise Devigne, François Pasteau, Marie Babel, et al.. A generic power wheelchair lumped model in the sagittal plane: towards realistic self-motion perception in a virtual reality simulator. ICRA 2023 - IEEE International Conference on Robotics and Automation, IEEE, May 2023, Londres, United Kingdom. pp.1-6. <hal-04044201>

**HAL Id: hal-04044201**

**<https://hal.science/hal-04044201v1>**

Submitted on 24 Mar 2023

**HAL** is a multi-disciplinary open access archive for the deposit and dissemination of scientific research documents, whether they are published or not. The documents may come from teaching and research institutions in France or abroad, or from public or private research centers.

L'archive ouverte pluridisciplinaire **HAL**, est destinée au dépôt et à la diffusion de documents scientifiques de niveau recherche, publiés ou non, émanant des établissements d'enseignement et de recherche français ou étrangers, des laboratoires publics ou privés.



Distributed under a Creative Commons CC BY 4.0 - Attribution - International License

# A generic power wheelchair lumped model in the sagittal plane: towards realistic self-motion perception in a virtual reality simulator

Fabien Grzeskowiak<sup>1</sup>, Ronan Le Breton<sup>2</sup>, Louise Devigne<sup>3</sup>, François Pasteau<sup>1</sup>, Marie Babel<sup>1</sup>, Sylvain Guégan<sup>2</sup>

**Abstract**—This paper presents a generic power wheelchair dynamic model. As a first contribution, this paper proposes to use a generic model composed of a geometric model and a lumped model in order to be compliant with a wide range of existing commercially available wheelchairs. In this model, a set of essential parameters are enough to accurately replicate the dynamic behavior of a wheelchair. As a second contribution, this paper presents an identification method of a n-wheel type power wheelchair. The presented model is restricted to the sagittal plane only, which is sufficient to study the reliability of the identification and validation methods. Moreover, a Motion Cueing Algorithm based on the proposed model controls a simulator mechanical platform. The generic model has been then validated through a user study with 18 able-bodied participants evaluating the self-motion perception with our multisensory power wheelchair driving simulator. Results show that the simplified model is sufficient to provide accurate sensations to the user with respect to their experience while driving a power wheelchair.

**Index Terms**—power wheelchair, assistive technology, lumped-model, system identification, user study, VR.

## I. INTRODUCTION

Driving simulation is a multisensory interactive application that aims to reproduce the driving experience with a real urban vehicle. The main objective of such simulators is to safely train people until they acquire enough skills to practice on a real vehicle. In the case of power wheelchair (PW) driving, training and repeated practice are mandatory to acquire driving skills, and thus to obtain PW prescription from therapists. For any type of vehicle, driving requires good visual, visuo-spatial and cognitive abilities. Unfortunately, these abilities can be too impaired for some people with neurological impairments to be able to train PW driving, as vehicle operation is too dangerous, even under supervision. PW simulation can provide these people with appropriate training in complete safety, until they acquire sufficient driving skills to train with a real PW [1].

The self-perception of our own movements through space relies on our ability to process a combination of auditory, visual, vestibular and proprioceptive sensory inputs. Therefore, vehicle simulators are a combination of motion and audiovisual platforms. While audiovisual cues can be provided by a HMD (Head-Mounted Display) and rely on software development, vestibular and haptic cues are provided by means of complex mechanical platforms with physical

limitations due to their structure, such as limited reachable workspace and the inability for the actuators to replicate large accelerations. Therefore, the motion generated by a simulator is generally different from the motion expected by its user because of these technological restrictions. Then, the reproduction of self-motion perception is a key strategy to reach perceptual validity [2]. Indeed, a simulator should provide high-fidelity motion cues to simulate vehicle motion and provide the user with high-quality self-motion perception. The control of these motion platforms then requires Motion Cueing Algorithms (MCA) to provide accurate self-motion perception to the user while making a trade-off with the physical constraints of the system [3].

In the case of a PW, the vehicle is 2-wheel differential drive platform which requires for each user to customize the seat and controllers, but also its dynamic parameters via programmable profiles. Several works tackle the modeling of a PW, but usually with PW-like robots (with custom electronics and motors) and not with commercially available PW [4] [5]. However, commercially available PW are adapted and customized for each user needs and characteristics. This heterogeneity would require a fine identification of numerous parameters to achieve an accurate modeling. Such identification on each different PW model and configuration would be tedious and inefficient. Yet, a generic model of PW motion behaviour needs to be defined based on a set of essential parameters able to fully characterize the system.

Lumped models are often used in the wheelchairs literature as a generic model. Indeed, in [6] authors propose a human-PW lumped model to design a dynamic absorber to compensate for the vertical vibration effects due to road excitation. This lumped model is then restricted to heave motion with a single spring mass-damper connection to the floor and the user is represented by a mass connected to the base of the PW with a spring mass-damper system. Another human-PW lumped model is proposed in [7] without defining a model for the human which is simply represented by a mass on the PW. This lumped model relies on a half-car approach. Another half-car approach lumped model is proposed by [8] for a manual wheelchair, where the user is represented by an additional lumped model connecting head and body. However, these lumped models are used to study vibration effects only.

This paper proposes then to use such a model as an input of the MCA in order to control the mechanical platform of a PW simulator, a compact 4 DoF mechanical platform which meets clinicians and end-users requirements [9] and simulate any type of PW. The objective of the proposed model is that

<sup>1</sup>Univ Rennes, INSA Rennes, Inria, CNRS, IRISA - UMR 6074, F-35000 Rennes, France, [fabien.grzeskowiak@insa-rennes.fr](mailto:fabien.grzeskowiak@insa-rennes.fr)

<sup>2</sup>Univ Rennes, INSA Rennes, LGCGM, F-35000 Rennes, France [sylvain.guegan@insa-rennes.fr](mailto:sylvain.guegan@insa-rennes.fr)

<sup>3</sup>Univ Rennes, Inria, CNRS, IRISA - UMR 6074, F-35000 Rennes, France

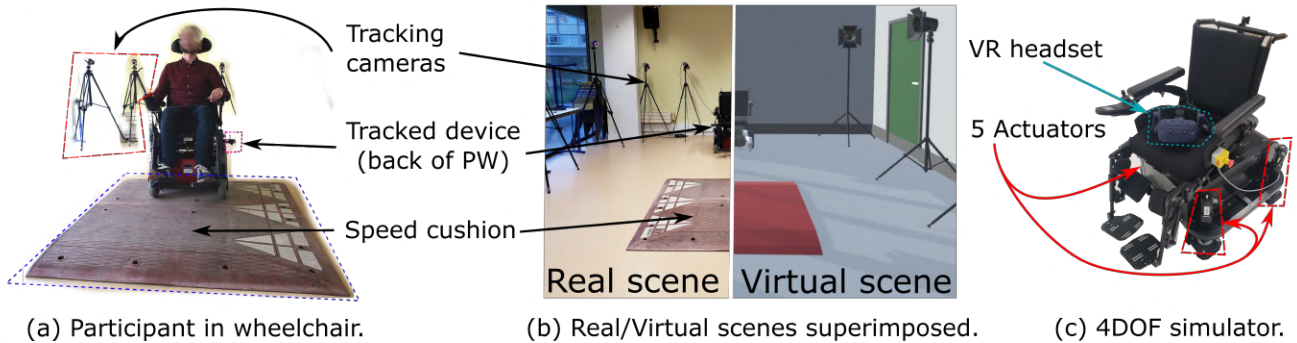


Fig. 1: Experimental setup. Participants were either on the wheelchair riding on a speed cushion (a) (b), or immersed in a similar scene in virtual reality (b) (c).

the user self-motion perception in simulation matches the one with a real PW. In an iterative process, this initial study focus on the sagittal plane.

The contributions of this paper are:

- a lumped model representation in the sagittal plane of a n-wheels PW including a minimal set of parameters;
- an identification method to fit the lumped model parameters to a real PW;
- a user study that validate the use of the lumped model as an input of the MCA in our PW immersive simulator.

The remainder of the article is as follows. First, we determine the key elements of the chosen Motion Cueing Algorithm in section II. Then, we present a lumped model and identify its essential parameters in section III. An experiment with participants is presented in section V. Finally, we draw guidelines for future work in section VI.

## II. SIMULATOR MOTION CUES

PW driving simulation is performed with a combination of motion and audiovisual platforms. Our multisensory PW simulator is composed of a 4 DoF motion platform with 5 actuators (Fig. 1) and a software framework compatible with any visual and auditory feedback platforms [9]. Its mechanical platform is designed so that any commercially available PW seat can be attached with the same mountings, thus allowing appropriate seating customization for any user.

In order to provide PW motion perception to the user, the actuators are controlled with a Motion Cueing Algorithm (MCA). This algorithm tackles both the mechanical platform motion and the rendering of visual cues through visual feedback interfaces.

In the field of vehicle simulation, there exist several Motion Cues Algorithms that are commonly used to control vehicle simulators [3]. The first MCAs that have been developed are washout algorithms [10]. They consist of scaling, filtering and tilt-coordination and became a reference widely used in the field because of their relative simplicity and reasonable performance. [11] have proposed other strategies such as MCA based on Optimal Control which integrate a mathematical model of the human vestibular system. In [12]

[13], a Model Predictive Control (MPC) has been proposed in order to improve the realism of motions produced by the platform, taking into account its workspace, where the algorithm parameters are set for the worst case scenario. In [2], authors present an objective method for assessing the perceptual fidelity of motion in vehicle simulators. [14] has proposed a methodology to implement classical MCA in discrete time recursive equations. In the literature of PW simulators, there are few works on MCA. In [15], a PW is disposed on a Gough-Stewart mechatronic platform, and a MPC-based MCA approach is proposed to efficiently optimize the motions of the platform.

In this paper, we propose to implement a MCA dedicated to a PW simulator based on washout algorithm, which is simple and computationally efficient [16]. The implementation follows the recommendations detailed in [17]. This paper's objective is to demonstrate that a generic PW lumped model is sufficient for this MCA to provide realistic self-motion perception.

## III. MODELING

In this paper, we propose a generic modeling for all types of PW. The proposed model is limited to the PW mobile base (*i.e.* from the wheel to the seat mountings) since we do not need to model the seat motion as our simulator platform can be fitted with any commercially available PW seat.

The proposed model is composed of two parts:

- a PW Geometric Model (GM) which represents the wheels and the suspension articulation system ;
- a Lumped Model (LM) which represents the PW dynamic behavior.

### A. Geometric model

The proposed Geometric Model (GM) for a 6-wheel PW is represented in the sagittal plane in Fig. 2 and defines:

- $(O_{world}, x, z)$  the world reference frame in the sagittal plane ;
- $O_i$  with  $i$  from 1 to  $n$  and  $n$  the number of contact points of each wheel in the sagittal plane according to the world reference frame ;

- $O_{GM}$  the output of the geometric model ;
- $(O_{GM}, x_{GM}, z_{GM})$  the PW frame attached to  $O_{GM}$  ;
- $\theta_{GM}$  the orientation of the frame  $(O_{GM}, x_{GM}, z_{GM})$  with respect to the  $(O_{world}, x, z)$  frame ;
- $Z_{GM}$  the altitude of the center of mass in the world frame.

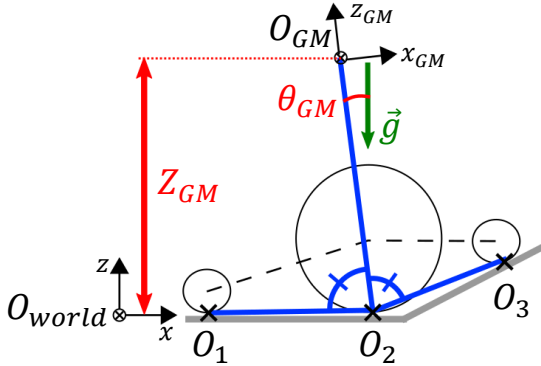


Fig. 2: PW Geometric Model: example with a 6-wheels PW.

The purpose of the GM is to estimate  $\theta_{GM}$  and  $Z_{GM}$  shown on Fig. 2 regardless of the type of PW used.

The estimators are defined as:

$$\hat{Z}_{GM} = \sum_{i=1}^n \alpha_i Z_{O_i} \quad (1)$$

$$\hat{\theta}_{GM} = \sum_{i=1}^{n-1} \sum_{j=i+1}^n \beta_{ij} \arcsin \left( \frac{Z_{O_i} - Z_{O_j}}{dx_{ij}} \right) \quad (2)$$

where  $\alpha_i$  and  $\beta_{ij}$  are related to the suspension architecture of the PW used and are experimentally identified,  $Z_{O_i}$  the altitude of the wheel contact point in the  $O_{world}$  frame,  $dx_{ij}$  the distance between the contact points of the wheels, and  $d_{C_M}$  is a constant value given by the altitude of the center of mass when the PW is on a flat plane.

### B. Lumped model

A lumped model simplifies the description of the physical system behavior. This model is used to facilitate the calculation, so the complexity of geometry can be ignored.

For the sake of simplicity, this paper presents the relevance of the LM assuming that the PW always maintains its motion in the sagittal plane corresponding to the  $X - Z$  plane of the PW (Fig. 2), *i.e.* the influence of axial perturbation or deflection to the motion of the PW is not considered in the proposed model.

We here propose a kinematic chain composed of a linear spring mass-damper system for the heave effects and a torsional spring mass-damper for the pitch effects. The PW model is therefore simplified in a 2 mass spring damper system.

Fig. 3 represents our dynamic model, as the extension of the GM defined in Fig. 2. Fig. 3 shows simplified LM according to  $Z$  and according to  $\theta$ , in series, taking as input the GM frame  $(O_{GM}, x_{GM}, z_{GM})$  and having as output the center of mass frame  $(C_M, x_M, z_M)$  attached to the center

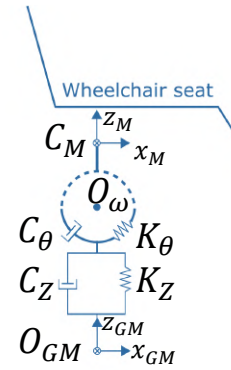


Fig. 3: PW Lumped Model.

of mass  $C_M$  in the sagittal plane. We here define the LM parameters  $K_\theta$ ,  $C_\theta$ ,  $K_Z$ , and  $C_Z$  as the stiffness and damping value according to  $Z$  and  $\theta$  respectively.

We define the motion equations of the PW model by using Newton's second law. It yields the familiar equation of motion

$$\mathbf{M}\ddot{\mathbf{X}}_M + \mathbf{C}(\dot{\mathbf{X}}_M - \dot{\mathbf{X}}_{GM}) + \mathbf{K}(\mathbf{X}_M - \mathbf{X}_{GM}) = \mathbf{F} \quad (3)$$

with  $\mathbf{X}_{GM} = [Z_{GM}(t) \ \theta_{GM}(t)]^T$  the output of the GM,  $\mathbf{X}_M = [Z_M(t) \ \theta_M(t)]^T$  the output of the LM,  $\mathbf{F} = [0 \ \Gamma_\theta(t)]^T$  the external forces applied on the PW,  $\mathbf{M} = \begin{bmatrix} M & 0 \\ 0 & J \end{bmatrix}$  the mass matrix of the PW,  $\mathbf{C} = \begin{bmatrix} C_Z & 0 \\ 0 & C_\theta \end{bmatrix}$  the damping matrix and  $\mathbf{K} = \begin{bmatrix} K_Z & 0 \\ 0 & K_\theta \end{bmatrix}$  the stiffness matrix.

## IV. IDENTIFICATION

The GM and the LM are identified using the same experimental protocol. An experiment with the PW is performed to identify the LM parameters defined in equation (3). The purpose of this experiment is to measure the PW motion in order to identify  $\mathbf{K}$ ,  $\mathbf{C}$  and  $\mathbf{M}$ .

$M$  consists of the moving mass of the PW ( $M_0$ ) and the mass of the user ( $M_u$ )

$$M = M_0 + M_u. \quad (4)$$

The moment of inertia  $J$  depends on the moment of inertia of the PW ( $J_0$ ), the moving mass  $M$  and the position of the centre of mass ( $d_{C_M}$ ) along  $z_m$

$$J = J_0 + d_{C_M}^2 M. \quad (5)$$

$d_{C_M}$  depends on the mass of the person seated on the PW chair. [18] and [19] proposed an experimental method to determine the center of mass and the moment of inertia. For this work, we followed their suggestion to approximate the position of the center of mass  $C_M$  as defined on Fig. 3, under the seat of PW.

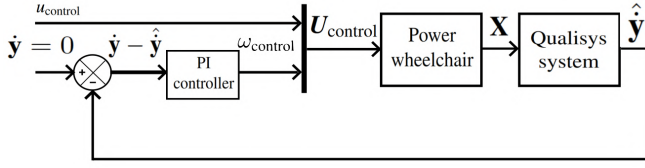


Fig. 4: Straight line servoing block diagram: a proportional integral correction targeting zero-speed on the y-axis is used.

1) *Hypotheses*: The mass loaded on the PW has effects only on the inertia of the PW. It has no effect on the PW speed as the PW manufacturer power module controller is designed to adapt torque to maintain speed, *i.e.* the defined forward speed is always reached regardless the external perturbations applied on the PW.

We considered 2 independent degrees of freedom  $Z$  and  $\theta$ , however, the damper and spring of each degree of freedom refer to the same suspension system.

2) *Experimental setup*: The experiment consists in applying autonomous control to the PW to maintain a linear trajectory on a path with a speed cushion so that there are 3 motion steps: acceleration on flat floor, constant speed on the speed cushion portion, and deceleration on flat floor. The setup is shown in Fig. 1. The PW power module have programmable profiles which allows to configure velocity and acceleration. The measurements were done with 28 different profiles from  $0.6 \text{ m.s}^{-1}$  to  $2.4 \text{ m.s}^{-1}$ . For each profile, we perform 5 tests each time for 6 conditions, *i.e.* with or without a speed cushion on the PW path with different loads  $M_u$  on the PW (0kg, 50kg, and 100kg).

The PW trajectory is measured with the motion capture system Qualisys which consists of 12 high speed infrared tracking cameras and a set of passive markers attached to the PW frame. The PW autonomously follows a strictly straight trajectory. We compensate the possible PW drifting effects by means of a corrector shown on Fig. 4. On this figure  $u_{\text{control}}$  is the speed selected for the trial,  $\dot{y}$  is the targeted zero-speed in y direction,  $\omega_{\text{control}}$  is the rotation control given to the PW after correction,  $U_{\text{control}}$  is the control vector combining  $u_{\text{control}}$  and  $\omega_{\text{control}}$ ,  $\mathbf{X}$  is the state of the PW and  $\hat{y}$  is the estimated y position of the PW given by the Qualisys tracking system.

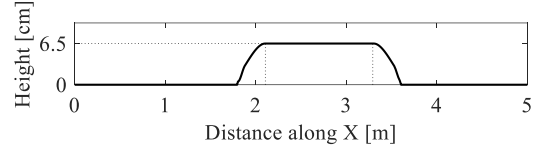
The GM parameters were identified with the set of measurements with lower speed ( $0.6 \text{ m.s}^{-1}$ ) in order to neglect the dynamic effects, and the LM parameters were identified with the set of measurements with higher speed ( $2.4 \text{ m.s}^{-1}$ ). The LM is identified using a state space approach in the time domain using an iterative rational function estimation approach [20]. We identified  $K_Z$  and  $C_Z$  using our identification data set along the  $Z$  axis. We used the same identified values of natural frequency and damping ratio for  $K_\theta$  and  $C_\theta$  as they refer to the same suspension system.

Table I shows the identified parameters.

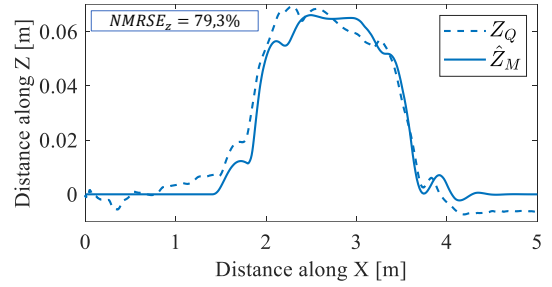
3) *Model validation*: Fig. 5b and Fig. 5c shows the identified model overlaying the validation data from the tests carried out at speed of  $1.2 \text{ m.s}^{-1}$  and a user mass of 100 kg.

$\alpha_1$	0.17	$\alpha_2$	0.66
$\alpha_3$	0.17	$\beta_{13}$	0
$\beta_{12}$	0.5	$\beta_{23}$	0.6
$dx_{12}$	0.38 m	$dx_{23}$	0.38 m
$dx_{23}$	0.76 m	$d_{C_M}$	0.43 m
$K_Z$	$4.18e^4 \text{ N/m}$	$K_\theta$	$1.04e^4 \text{ N.m/rad}$
$C_Z$	$2.24e^3 \text{ N.s/m}$	$C_\theta$	$5.6e^2 \text{ N.m.s/rad}$
$M_0$	53 kg.N/m	$J_0$	$9.9 \text{ kg.m}^2$

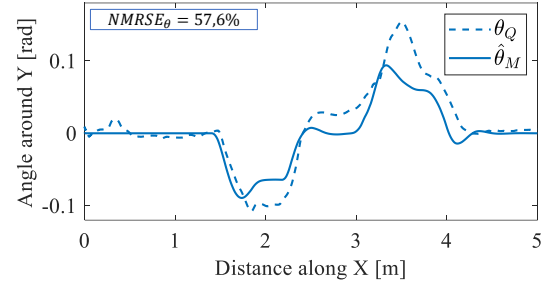
TABLE I: Identified essential geometric and dynamic parameters of PW



(a) Geometry of the speed cushion, *i.e.* the model input



(b) Comparison along  $Z$  degree of freedom.  $Z$  values are centered to 0 at the beginning of the trial to ease comparison between curves.



(c) Comparison along  $\theta$  degree of freedom.

Fig. 5: Comparison of models and experimental data at forward speed of  $1.2 \text{ m.s}^{-1}$ . Dashed line is ground truth from validation data (Qualisys measurements –  $Z_Q$  and  $\theta_Q$ ). Solid line is global model (GM + LM –  $\hat{Z}_M$  and  $\hat{\theta}_M$ ).

We use the normalized root mean square error to evaluate the fitness of our model. We observe that the Fig. 5b referring to the degree of freedom  $Z$  shows properly fitted curves, with  $NRMSE_z = 100 \left( 1 - \frac{\|Z_Q - \hat{Z}_M\|}{\|Z_Q - Z_Q\|} \right)$  giving a fitness value indicator of 79.3% while on Fig. 5c referring to the  $\theta$  degree of freedom, the model appear to be scaled down with a  $NRMSE_\theta$  fitness value indicator of 57.6% .

This identification require further validation. Fig. 6 shows the validation workflows for the identification. On Fig. 6a, tracking data are used as input for the MCA, while on Fig. 6b, data are reconstructed with the model. On Fig. 6a, Qualisys measurements output a state of the center of mass which is directly injected in the MCA. On Fig. 6b, the  $X_Q$

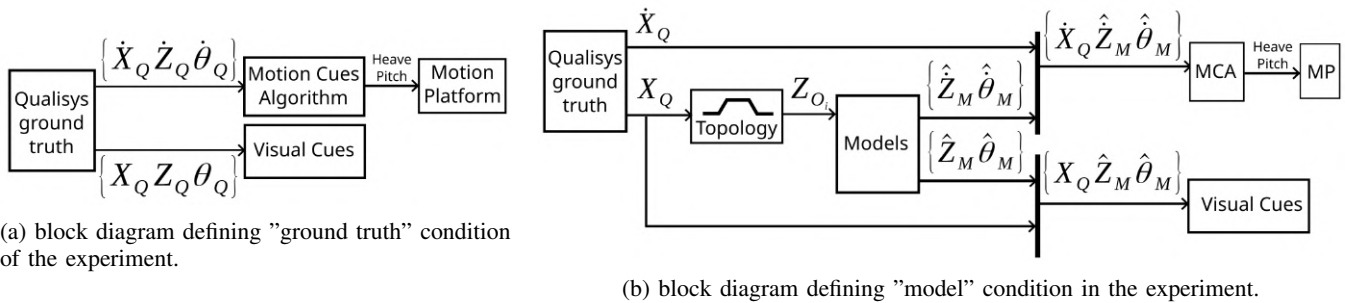


Fig. 6: Block diagrams defining our two experimental conditions.

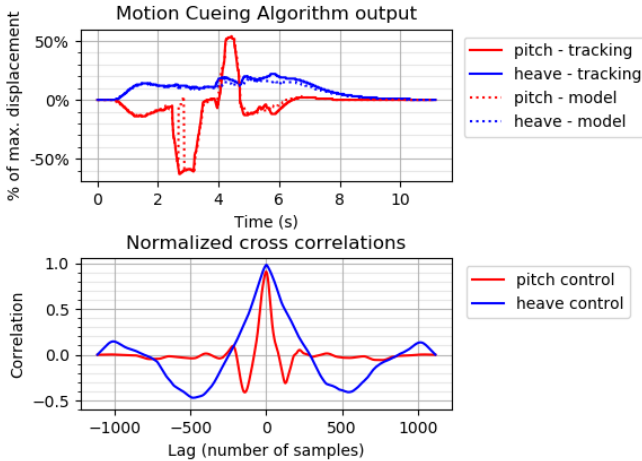


Fig. 7: Comparison of MCA outputs with model data and tracking data.

input from ground truth data is given in a topology block which generate the  $Z_{O_i}$  component for each wheel, which is then given to the model which generates an estimated state  $(\hat{Z}, \hat{Z}, \hat{\theta}, \hat{\theta})$  of the center of mass. This partial state is associated to the X input and fed in the visual cues block and in the MCA. On both Fig. 6, the MCA generates heave and pitch control signals to be used by the motion platform (MP).

The Fig. 7 shows a comparison between the MCA outputs when either ground truth validation data or model data are used and provides the related cross correlation. The main difference between the two conditions occurs at time=3s, and corresponds to the first peak shown on Fig. 5c ( $X = 1.8$  m). This corresponds to the moment where the caster wheel is in contact with the cushion: our model considers the cushion as infinitely rigid, leading to relatively high reaction of the MCA.

## V. USER PERCEPTION STUDY

### A. Objectives and hypotheses

A user perception study has been conducted in order to validate our PW model. Our hypothesis is that the model is accurate enough to provide the proper sensations to the users of our simulator. The experiment consists in asking participants to evaluate the quality of their sensations in

the PW simulator in two conditions: in the PW simulator using data captured with the real PW, and with the PW simulator using data generated by the generic PW model. The objective is to evaluate the quality of the PW state generated by the generic PW model when compared to the PW state extracted from motion capture through the motion cues of the simulator. For all conditions, the PW profile was set to  $1.2 \text{ m.s}^{-1}$ , as it is a good representation of a typical indoor navigation.

### B. Participants

18 people participated to our study. All subjects were from INSA Rennes (employee or students) who volunteered for the study. They gave their informed consent. The protocol has been validated through "Inria Coerle" ethic comity.

### C. Procedure

In an initial step, participants could get used to a PW and focus on their perceptions during a predefined trajectory. Then the PW were positioned on a marker in the room. The control algorithm shown on Fig. 4 was used to perform a straight linear motion of the PW with the user. They could use the joystick as a dead-man switch and had no other control over the PW. The set up is shown on Fig. 1.

1) *Tasks*: The participants were immersed in the virtual room shown on Fig. 1 and could look around to get used to the virtual environment. They were sitting on our PW simulator wearing a head mounted display as shown in Fig. 1. Once they were ready we simulate a pair of trials, the virtual PW is likewise autonomously controlled. The virtual PW followed either a trajectory corresponding to measurements of the real PW (condition  $T_r$  Fig. 6a), or a trajectory generated by the generic PW model (condition  $T_m$  Fig. 6b). Conditions  $T_r$  and  $T_m$  were randomized. Participants were asked to focus on their sensations to compare them with their earlier sensations in the real PW, thanks to a questionnaire.

2) *Questionnaire*: We used a decision tree with descriptors leading to numerical ratings (Fig. 8a) based on the same structure as the established Cooper-Harper HQR scale [21], but streamlined to fit our application. The decision tree guides the participant to evaluate his or her experience with a numerical rating between 1 and 6: a rating of 1 indicates that the motion cues are consistent with reality, the sensations are close to reality, and there are insignificant

impairments; a rating of 5 indicates that the motion cues are not acceptable, that there are obvious deficiencies leading to total disorientation. A score of 6 does not mean that this is the worst possible configuration, but simply that no signal was perceived.

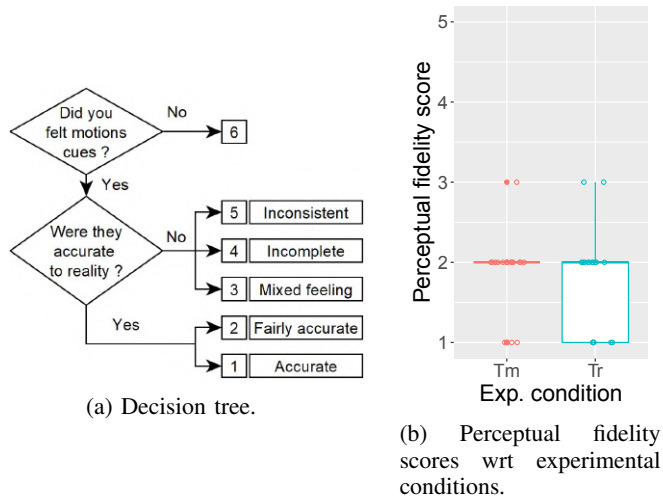


Fig. 8: Decision tree (a) used to guide participants to rate their feeling after each trial in simulation and results (b) as a boxplot from the questionnaire using (a). The boxplot gives the median, 25 and 75 percentiles with extrema values.

#### D. Results

Results are given in boxplot diagrams which represent the score given by each participant for the different experimental conditions (Fig. 8b).

Each participant felt sensations in the simulator (no one gave a score of 6), and 95% of the participants gave either a score of 1 ("Accurate") or 2 ("Fairly accurate") for each condition (max. value is 3: "Mixed Feeling"). Mean values were found at 1.89 (Med: 2) for condition  $T_m$  and at 1.78 (Med: 2) for condition  $T_r$ . Scores values were not normally distributed (Shapiro-Wilk normality tests) and matched-paired Wilcoxon test showed no significant differences between the two conditions ( $p = 0.5045$ ,  $W = 180$ ). This suggests that the motion rendered by our model leads to a realistic motion perception, similar to the one obtained with ground truth data.

## VI. DISCUSSION

The results on Fig. 7 show the different MCA outputs generated thanks to respectively the model and the tracking data corresponding to the ground truth, and compare them using cross correlation. When synchronizing both signals, the cross correlation is maximal for heave control and pitch control, displaying values higher than 0.98. This result shows the high level of similarities between the model based signal and the tracking data based signal. To complete the validation of our model, a user study was conducted in section V which showed that the participants perceived accurate motions with respect to the reality. The PW motions (real and virtual)

were autonomous so that each participant experienced the same conditions. Regarding the score given by participants to each condition, the statistical analysis shows that there is not a significant difference between the "tracking data" condition  $T_r$  and the "model based data" condition  $T_m$ . This results shows a similarity between the two conditions in terms of perception. This fully validates the identification presented in section IV. These results are in accordance with our assumption: the model is accurate enough to be used in simulation.

In the future, we would like to expand the lumped model of the PW to all degrees of freedom, and to extend it to take into account caster wheel behavior. If we have restricted the study to 6-wheels wheelchairs, our approach is suitable to other types of wheelchairs, such as 4-wheels wheelchairs with propulsion or traction. In addition, we plan to determine a more specific Motion Cueing Algorithm of our simulator in order to improve participant experience. Finally, we are planning experiments where the participants will drive by themselves the PW (real and virtual) in a circuit. In addition, it would be interesting to use physiological measurement devices (EMG, EEG, GSR...) to evaluate the attention and cognitive cost.

## VII. CONCLUSION

This paper proposes a generic lumped model of power wheelchair whose purpose is to serve as an input for a Motion Cueing Algorithm (MCA) controlling a power wheelchair simulator. This paper describes this model restricted to the sagittal plane. The accuracy of such model has been investigated by the means of a user perception study. The model was first identified with respect to a real power wheelchair. The identification was validated using cross correlation when comparing the MCA outputs between the model and ground truth data. The model was then used in a user perception study. The participants of the study were asked to focus on their sensations in the simulator along with two conditions: the simulator was either controlled by a ground truth tracking based dataset, either by a model based dataset. The results of this study show that there is no difference between the two conditions in terms of sensations. Therefore, we can consider the proposed model to be accurate enough to be used in our simulation. In addition, our model can be easily extended to any type of power wheelchair (rear, middle, front drive wheels), and to integrate additional degrees of freedom. These issues will be addressed in future works.

## ACKNOWLEDGMENT

This work is carried out as part of the INTERREG VA FMA ADAPT project "Assistive Devices for empowering disABled People through robotic Technologies" (adapt-project.com). The Interreg FCE Programme is a European Territorial Cooperation programme that aims to fund high quality cooperation projects in the Channel border region between France and England. The Programme is funded by the European Regional Development Fund (ERDF).

## REFERENCES

- [1] S. Arlati, V. Colombo, G. Ferrigno, R. Sacchetti, and M. Sacco, "Virtual reality-based wheelchair simulators: A scoping review," *Assistive Technology*, vol. 32, no. 6, pp. 294–305, 2020.
- [2] S. Casas-Yrurzum, C. Portales-Ricart, P. Morillo-Tena, and C. Cruz-Neira, "On the objective evaluation of motion cueing in vehicle simulations," *IEEE Transactions on Intelligent Transportation Systems*, vol. 22, pp. 3001–3013, May 2021.
- [3] S. Casas, R. Olanda, and N. Dey, "Motion cueing algorithms: A review: Algorithms, evaluation and tuning," *International Journal of Virtual and Augmented Reality*, pp. 90–106, October 2017.
- [4] D. Herrera, F. Roberti, R. Carelli, V. Andaluz, J. Varela, J. Ortiz, and P. Canseco, "Modeling and path-following control of a wheelchair in human-shared environments," *International Journal of Humanoid Robotics*, vol. 15, April 2018.
- [5] J. S. Ortiz, G. Palacios-navarro, V. H. Andaluz, and L. F. Recalde, "Three-dimensional unified motion control of a robotic standing wheelchair for rehabilitation purposes," *Sensors*, vol. 21, May 2021.
- [6] S. Wang, L. Zhao, Y. Hu, and F. Yang, "Vibration characteristics analysis of convalescent-wheelchair robots equipped with dynamic absorbers," *Hindawi Shock and Vibration*, 2018.
- [7] J. L. Candiotti, A. Neti, S. Sivakanthan, and R. A. Cooper, "Analysis of whole-body vibration using electric powered wheelchairs on surface transitions," *MDPI Vibration*, vol. 5, pp. 98–109, January 2022.
- [8] M. F. Hikmawan and A. S. Nugraha, "Analysis of electric wheelchair passenger comfort with a half car model approach," in *2016 IEEE International Conference on Sustainable Energy Engineering and Application: Sustainable Energy for a Better Life (ICSEEA)*, pp. 76–80, 2016.
- [9] G. Vailland, F. Grzeskowiak, L. Devigne, Y. Gaffary, B. Fraudet, E. Leblong, F. Nouviale, F. Pasteau, R. Le Breton, S. Guegan, *et al.*, "User-centered design of a multisensory power wheelchair simulator: towards training and rehabilitation applications," in *IEEE 16th International Conference on Rehabilitation Robotics (ICORR)*, IEEE, June 2019, pp. 77–82.
- [10] S. Schmidt and B. Conrad, "The calculation of motion drive signals for piloted flight simulators," Tech. Rep., (Rep. No. 69-17). Palo Alto, CA, NASA, 1969.
- [11] P. Duc-An and N. Duc-Toan, "A novel motion cueing algorithm integrated multi-sensory system—vestibular and proprioceptive system," *Proceedings of the Institution of Mechanical Engineers, Part K: Journal of Multi-body Dynamics*, vol. 234, pp. 256–271, June 2020.
- [12] Y. R. Khusro, Y. Zheng, M. Grotoli, and B. Shyrokau, "Mpc-based motion-cueing algorithm for a 6-dof driving simulator with actuator constraints," *Vehicles*, vol. 2, pp. 625–647, December 2020.
- [13] C. Rengifo, J. R. Chardonnet, H. Mohellebi, and A. Kemeny, "Impact of human-centered vestibular system model for motion control in a driving simulator," *IEEE Transactions on Human-Machine Systems*, vol. 51, pp. 411–420, October 2021.
- [14] A. Sharma, M. S. Ikbali, and M. Zoppi, "Acausal approach to motion cueing," *IEEE Robotics and Automation Letters*, vol. 4, pp. 1013–1020, April 2019.
- [15] L. A. Dao, A. Prini, M. Malosio, A. Davalli, and M. Sacco, "A mixed-integer model predictive control approach to motion cueing in immersive wheelchair simulator," in *IEEE/RSJ International Conference on Intelligent Robots and Systems (IROS)*, October 2020, pp. 4161–4167.
- [16] M. A. Nahon and L. D. Reid, "Simulator motion-drive algorithms - a designer's perspective," *Journal of Guidance, Control, and Dynamics*, vol. 13, no. 2, pp. 356–362, 1990.
- [17] G. Reymond and A. Kemeny, "Motion cueing in the renauld driving simulator," *Vehicle System Dynamics*, vol. 34, no. 4, pp. 249–259, 2000.
- [18] X. Chen, J. G. Chase, P. Wolm, I. Anstis, J. Oldridge, W. Hanbury-Webber, R. Elliot, and W. Pettigrew, "System identification and modelling of front wheel drive electric wheelchairs," *IFAC Proceedings Volumes*, vol. 41, pp. 3076–3081, 2008.
- [19] B. R. Cho, J. Y. Yoon, S. Kho, J. I. Lee, S. O. Kwon, H. K. An, S. Lee, and C. Kim, "Seat posture stabilizing function for an electric wheelchair based on controlled pendulum mechanism," *4th International Conference on Control, Decision and Information Technologies (CoDIT)*, pp. 365–370, January 2017.
- [20] L. Ljung, *System Identification : Theory for the User*, 2nd ed. Prentice Hall PTR, 1999.
- [21] G. Cooper and R. Harper, "The use of pilot rating in the evaluation of aircraft handling qualities," Tech. Rep., NASA Technical Note, D-5153, April 1969.